Inhibition of soluble epoxide hydrolase attenuates a high-fat diet-mediated renal injury by activating PAX2 and AMPK

Ying Luo[a,b], Ming-Yu Wu[a,b], Bing-Qing Deng[a,b], Jian Huang[a,b], Sung Hee Hwang[c,d], Meng-Yuan Li[a,b], Chun-Yu Zhou[a,b], Qian-Yun Zhang[a,b], Hai-Bo Yu[a,b], Da-Ke Zhao[a,b], Guodong Zhang[e,f], Ling Qin[a,b], Ai Peng[a,b], Bruce D. Hammock[c,d,1], and Jun-Yan Liu[a,b,1]

[a]Center for Nephrology and Metabolomics, Shanghai Tenth People's Hospital, Tongji University School of Medicine, 200072 Shanghai, People's Republic of China; [b]Division of Nephrology and Rheumatology, Shanghai Tenth People's Hospital, Tongji University School of Medicine, 200072 Shanghai, People's Republic of China; [c]Department of Entomology and Nematology, University of California, Davis, CA 95616; [d]Comprehensive Cancer Center, University of California, Davis, CA 95616; [e]Department of Food Science, University of Massachusetts, Amherst, MA 01003; and [f]Molecular and Cellular Biology Graduate Program, University of Massachusetts, Amherst, MA 01003

Contributed by Bruce D. Hammock, January 25, 2019 (sent for review September 14, 2018; reviewed by A. Daniel Jones and Craig R. Lee)

A high-fat diet (HFD) causes obesity-associated morbidities involved in macroautophagy and chaperone-mediated autophagy (CMA). AMPK, the mediator of macroautophage, has been reported to be inactivated in HFD-caused renal injury. However, PAX2, the mediator for CMA, has not been reported in HFD-caused renal injury. Here we report that HFD-caused renal injury involved the inactivation of Pax2 and Ampk, and the activation of soluble epoxide hydrolase (sEH), in a murine model. Specifically, mice fed on an HFD for 2, 4, and 8 wk showed time-dependent renal injury, the significant decrease in renal Pax2 and Ampk at both mRNA and protein levels, and a significant increase in renal sEH at mRNA, protein, and molecular levels. Also, administration of an sEH inhibitor, 1-trifluoromethoxyphenyl-3-(1-propionylpiperidin-4-yl)urea, significantly attenuated the HFD-caused renal injury, decreased renal sEH consistently at mRNA and protein levels, modified the renal levels of sEH-mediated epoxyeicosatrienoic acids (EETs) and dihydroxyeicosatrienoic acids (DHETs) as expected, and increased renal Pax2 and Ampk at mRNA and/or protein levels. Furthermore, palmitic acid (PA) treatment caused significant increase in *Mcp-1*, and decrease in both Pax2 and Ampk in murine renal mesangial cells (mRMCs) time- and dose-dependently. Also, 14(15)-EET (a major substrate of sEH), but not its sEH-mediated metabolite 14,15-DHET, significantly reversed PA-induced increase in *Mcp-1*, and PA-induced decrease in Pax2 and Ampk. In addition, plasmid construction revealed that Pax2 may positively regulate Ampk transcriptionally in mRMCs. This study provides insights into and therapeutic target for the HFD-mediated renal injury.

metabolomics | autophagy | renal hypertrophy | eicosanoids | lipidomics

Mounting evidence supports that human health heavily depends on diet (1–3). A high-fat diet (HFD), in which the fat provides above 40% of daily caloric intake, is an important part of the modern western pattern diet (4, 5). In some cases, an HFD was reported to improve glycemic control (6), blood glucose control (7), cardiac function (8), and metabolic status (9). However, frequent and chronic consumption of an HFD is a well-known risk factor for obesity (10), diabetes (11), cancer (12), osteoarthritis (13), rheumatoid arthritis (14), stroke (15), cardiovascular disease (16), colonic inflammation (17), and multiple sclerosis (18). In addition, an HFD has been well documented to be a causative factor for fatty liver (19, 20) and renal dysfunction (21). Such renal dysfunction prompts the progression of chronic kidney disease, diabetic nephrology, and many other diseases mentioned above. Therefore, it's translationally and clinically significant to investigate the molecular mechanisms underlying HFD-mediated kidney injury and the associated intervention targets.

HFD-mediated kidney injury includes renal hypertrophy and functional abnormalities (21, 22), which may involve macroautophagy and chaperone-mediated autophagy (CMA) (23, 24). The 5′-adenosine monophosphate (AMP)-activated protein kinase (AMPK) is an important activator of macroautophagy by activating Unc-51–like autophagy activating kinase 1 (ULK1) (25), which has been documented to be inactivated in HFD-mediated renal injury (21, 26, 27). However, the function of paired box gene 2 (*PAX2*), the crucial mediator for CMA (28–30), has never been reported in HFD-mediated renal injury.

Recently, AMPK was reported to be activated by cytochrome P450 (CYP) 2J2 and its metabolites, such as epoxyeicosatrienoic acids (EETs), which contribute to the attenuation of cardiac injuries (31–33). EETs are not only the metabolites of arachidonic acid (ARA) mediated by CYP2C and CYP2J, but also the substrates for the enzyme soluble epoxide hydrolase (sEH, encoded by *EPHX2*) (34, 35). However, whether the EETs and their degradation by sEH alter AMPK activation in HFD-mediated renal injury remains unknown. In addition, given that PAX2 plays a role in HFD-mediated renal injury, the correlation of PAX2 with AMPK and EETs/sEH has not been investigated. Here we report that the inhibition of sEH attenuates HFD-mediated kidney injury through

Significance

This study reveals that the inactivation of Pax2, a mediator for chaperone-mediated autophagy, contributes to the high-fat diet (HFD)-caused murine renal injury. Also, the inactivation of Ampk, a mediator of macroautophagy, and the activation of soluble epoxide hydrolase (sEH), an enzyme mediating the metabolism of epoxy fatty acids to form vicinal diols, are involved in HFD-caused murine renal injury. Furthermore, inhibition of sEH significantly attenuates the HFD-induced renal injury, partially by activating Pax2 and Ampk. Increased epoxy fatty acids caused by sEH inhibition activate Pax2 and Ampk. In addition, Pax2 may upregulate Ampk transcriptionally in murine renal mesangial cells. This study provides insights into the pathophysiology and pharmacology of HFD/obesity-mediated renal injury.

Author contributions: J.-Y.L. designed research; Y.L., M.-Y.W., B.-Q.D., J.H., M.-Y.L., C.-Y.Z., Q.-Y.Z., H.-B.Y., D.-K.Z., and J.-Y.L. performed research; S.H.H. and B.D.H. contributed new reagents/analytic tools; Y.L., M.-Y.W., B.-Q.D., G.Z., L.Q., A.P., and J.-Y.L. analyzed data; and B.D.H. and J.-Y.L. wrote the paper.

Reviewers: A.D.J., Michigan State University; and C.R.L., University of North Carolina at Chapel Hill.

The authors declare no conflict of interest.

[1]To whom correspondence may be addressed. Email: bdhammock@ucdavis.edu or jyliu@tongji.edu.cn.

This article contains supporting information online at www.pnas.org/lookup/suppl/doi:10.1073/pnas.1815746116/-/DCSupplemental.

Published online February 25, 2019.

increased EETs activating Pax2 and Ampk in a murine model by using a metabolomics approach.

Results

HFD Caused Excessive Body Weight Gain in a Murine Model. As illustrated in *SI Appendix*, Fig. S1 *A–C*, the mice fed with an HFD gained significantly greater body mass than those fed on a control diet (CTD) after 1-wk feeding. In addition, the difference in the average body mass of the mice fed on an HFD and a CTD progressively increased with the treatment time.

HFD Caused Renal Hypertrophy and Renal Injury. The mice fed on an HFD for 2, 4, and 8 wk had a significantly greater renal mass (1.1-fold), ratio of renal mass to tibial length (1.1-fold), and renal level of *Ngal* (1.5- to ∼2.0-fold) (*SI Appendix*, Fig. S2 *A–C*) than those with a CTD. Compared with a CTD, intake of an HFD for 8 wk resulted in significantly higher renal levels of *Il-6* (1.5-fold) and *Mcp-1* (3.7-fold) and plasma level of creatinine (Cr) (1.15-fold) than in mice on a CTD (*SI Appendix*, Fig. S2 *D–F*). In addition, the mice fed on an HFD for 4 wk had a higher plasma level of urea nitrogen (UN) than those on a CTD. However, the plasma UN returned to the normal level when the mice were fed with an HFD for 8 wk (*SI Appendix*, Fig. S2*G*).

In addition, no visual difference was observed in the renal proximal tubular cells (RPTCs) from the mice fed with an HFD for 2 wk (*SI Appendix*, Fig. S3 *A–D*). However, vacuoles were visually observed in the RPTCs from the mice fed with an HFD for 4 wk (*SI Appendix*, Fig. S3 *E–H*), and still more vacuoles were visually observed in the kidney from the mice fed with an HFD for 8 wk (*SI Appendix*, Fig. S3 *I–L*). These vacuoles were caused by the loss of lipids that were stained by Periodic Acid Schiff.

HFD Reduced the Renal Levels of Dihydroxyeicosatrienoic Acids and EETs via Increasing sEH but Not Decreasing CYPs. The renal levels of lipid signaling mediators (LSMs) are summarized in *SI Appendix*, Table S1. A 2D scatter plot for the orthogonal partial least squares-discriminant analysis (OPLS-DA) of the renal LSMs from the mice treated for 8 wk visually separated the mice fed with an HFD from those with a CTD (Fig. 1*A*). The corresponding S plot (Fig. 1*B*) showed that 5,6-, 8,9-, and 11,12-dihydroxyeicosatrienoic acid (DHET) were the major factors that contributed to the difference between the mice fed on an HFD and a CTD. The renal levels of both the four DHET isomers and their EET precursors significantly decreased after 8-wk intake of an HFD (Fig. 1*C* and *SI Appendix*, Fig. S2*I*). However, 2- and 4-wk feeding with an HFD failed to modify renal levels of EETs (Fig. 1*D*) and DHETs (Fig. 1*E*) significantly. In addition, although HFD failed to modify the renal mRNA levels of *Cyp2c29*, *Cyp2c37*, *Cyp2c38*, *Cyp2c39*, *Cyp2c44*, *Cyp2j5*, and *Cyp2j6* (*SI Appendix*, Fig. S2*J*) significantly, it significantly increased the renal mRNA level of *Ephx2* (sEH) (∼twofold) after 4-wk feeding of an HFD (Fig. 1*I*). The renal protein level of sEH also significantly increased in the mice fed on an HFD for 8 wk compared with the mice with a CTD (*SI Appendix*, Fig. S4 *A* and *B*).

HFD Inactivated Pax2 and Ampk Time-Dependently. The renal mRNA level of *Pax2* (∼0.7-fold) was significantly decreased in the mice fed with an HFD for 4 wk (Fig. 1*G*). Also, the mRNA expression of *Ampk* (∼0.7-fold) in renal tissue was significantly lower for the mice fed on an HFD for 8 wk than for those treated with a CTD (Fig. 1*H*). In addition, the renal protein levels of Pax2 and p-Ampk$_\alpha$ (Thr172) significantly decreased in the mice fed on an HFD for 8 wk compared with those with a CTD (*SI Appendix*, Fig. S4 *C–F*).

Treatment with TPPU Attenuated HFD-Mediated Renal Injury. Treatment with 1-trifluoromethoxyphenyl-3-(1-propionylpiperidin-4-yl) urea (TPPU), a potent sEH inhibitor, significantly reduced the HFD-induced increase in renal *Mcp-1* (Fig. 2*A*), renal mass, ratio of renal mass to tibial length, renal *Ngal* and *Il-6* (*SI Appendix*, Fig. S5 *A–D*), and plasma Cr level (*SI Appendix*, Fig. S5*E*). In addition, TPPU treatment visibly reduced the HFD-induced increase in the vacuoles in RPTCs (*SI Appendix*, Fig. S6).

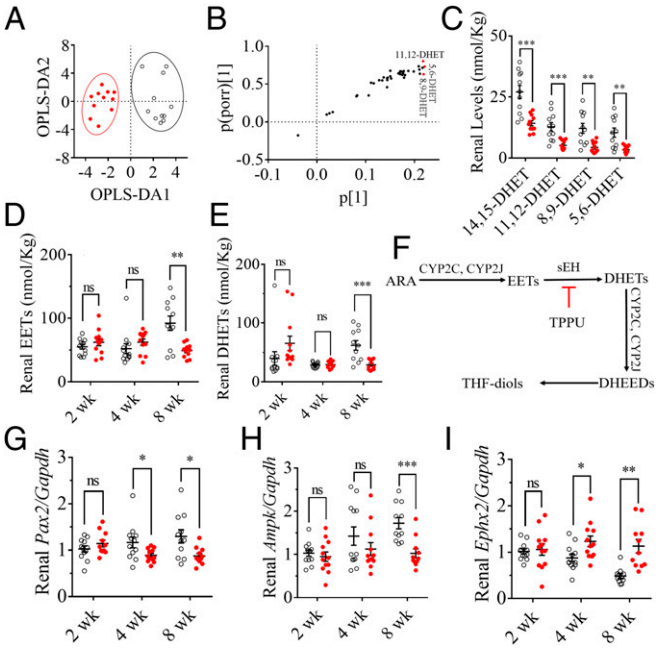

Fig. 1. An HFD caused murine renal injury involved in the activation of sEH and the inactivation of Ampk and Pax2. (*A*) A 2D scatter plot for OPLS-DA of the renal LSMs highlights the difference between the mice fed on an HFD (red dots) and a CTD (unfilled circles) for 8 wk. R2X = 0.791, R2Y = 0.780, and Q2 = 0.582. (*B*) S plot of the OPLS-DA model in *A* shows that 5,6-, 8,9-, and 11,12-DHET were the three major markers contributing to the discrimination of the mice fed with an HFD and a CTD (the VIP values are presented in *SI Appendix*, Table S1). (*C*) The 8-wk intake of HFD significantly decreased renal levels of 11,14-, 11,12-, 8,9-, and 5,6-DHET; the corresponding renal levels of 14(15)-, 11(12)-, 8(9)-, and 5(6)-EET are presented in *SI Appendix*, Fig. S2*E*. The renal levels of (*D*) total EETs [the sum of 14(15)-, 11(12)-, 8(9)-, and 5(6)-EET] and (*E*) total DHETs (the sum of 11,14-, 11,12-, 8,9-, and 5,6-DHET) were significantly decreased in the mice fed with an HFD for 8 wk but only slightly changed in the mice treated for 2 and 4 wk. (*F*) A brief scheme of the metabolic pathways for EETs and DHETs. (*G*) The renal *Pax2* were decreased transcriptionally by feeding HFD for 4 and 8 wk. (*H*) The renal *Ampk* were decreased transcriptionally by 8-wk intake of HFD. (*I*) The renal *Ephx2* were increased transcriptionally by feeding HFD for 4 and 8 wk; the data for HFD-caused renal injury are presented in *SI Appendix*, Fig. S2 *A–D*. The data represent mean ± SEM (n = 11 to ∼12); ns (no significant difference) $P \geq 0.05$, $0.01 < {*}P < 0.05$, $0.001 < {**}P \leq 0.01$, and $0.0001 < {***}P \leq 0.001$ were determined by two-tailed t test.

Treatment with TPPU Significantly Increased Renal EETs and Decreased Renal DHETs via Inhibiting sEH. TPPU treatment significantly reversed the HFD-induced decrease in the renal levels of 14(15)-, 11(12)-, 8(9)-, and 5(6)-EET (Fig. 2*B*), and decreased the renal levels of 11,12-, 8,9-, and 5,6-DHET significantly but of 14,15-DHET nonsignificantly (Fig. 2*C*). In addition, TPPU treatment significantly inhibited the HFD-induced increase in renal mRNA and protein levels of sEH (Fig. 2 *D–F*).

Treatment with TPPU Significantly Increased HFD-Inactivated Ampk and Pax2. The treatment of TPPU significantly increased the HFD-induced decrease in the renal mRNA level of *Ampk* (Fig. 2*G*) and renal protein level of p-Ampk$_\alpha$ (Fig. 2 *H* and *I*), respectively. In contrast, although TPPU treatment significantly decreased the HFD-induced decrease in renal mRNA level of *Pax2* (Fig. 2*J*), it significantly reversed the HFD-induced decrease in renal protein level of Pax2 and p-Pax2 (Ser393) (Fig. 2 *K* and *L* and *SI Appendix*, Fig. S7 *A* and *B*).

PHARMACOLOGY

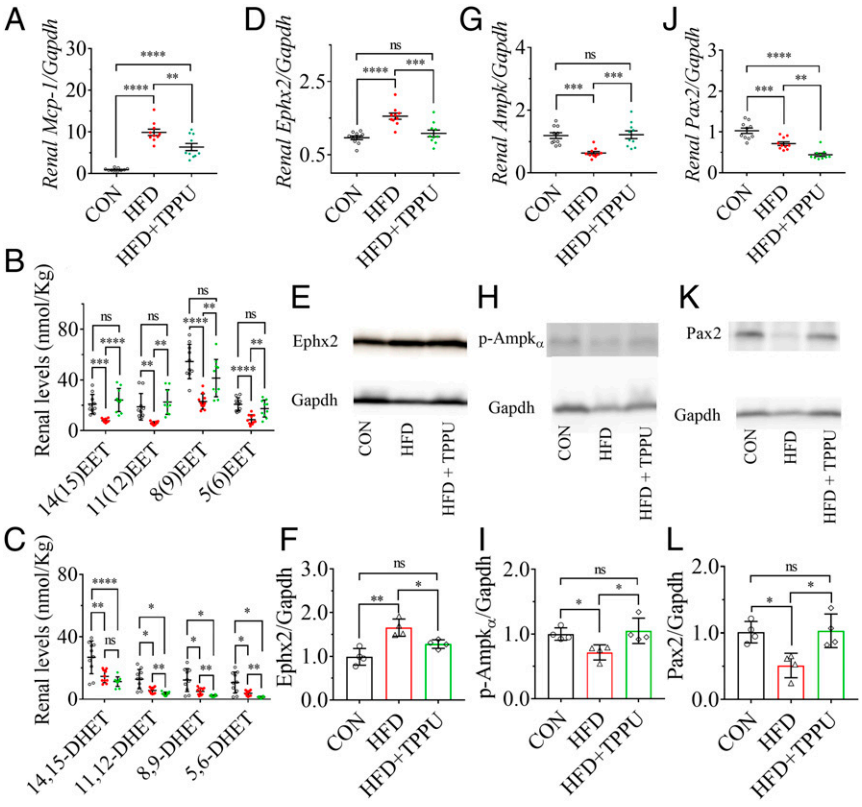

Fig. 2. Inhibition of sEH by pharmacological intervention with the sEH inhibitor TPPU attenuated the HFD-mediated renal injury by activating Pax2 and Ampk. (*A*) Treatment with TPPU significantly reduced the HFD-induced renal mRNA level of *Mcp-1*. (*B*) TPPU treatment markedly increased HFD-induced decrease in renal levels of 14(15)-, 11(12)-, 8(9)-, and 5(6)-EET while (*C*) TPPU significantly decreased HFD-induced decrease in renal levels of 11,12-, 8,9-, and 5,6-DHET. Renal mRNA levels of (*D*) *Ephx2*, (*G*) *Ampk*, and (*J*) *Pax2* were significantly modified by TPPU treatment; Western blot analysis and quantitation of the band density of (*E* and *F*) Ephx2, (*H* and *I*) p-Ampk$_\alpha$, and (*K* and *L*) Pax2. Unfilled circles, red dots, and green triangles represent the individual mouse treated with a CTD, an HFD, and an HFD with TPPU, respectively. Data represent mean ± SEM for *A*–*C*, *D*, *G*, and *J* (n = 10), and mean ± SD for *F*, *I*, and *L* (n = 4). The Western blot analysis and quantitation of the band density of p-Pax2 (Ser-393) is presented in *SI Appendix*, Fig. S7 *A* and *B*, which shows a similar pattern to Pax2; ns (no significant difference) $P \geq 0.05$, $0.01 < {*}P < 0.05$, $0.001 < {**}P \leq 0.01$, $0.0001 < {***}P \leq 0.001$, and ${****}P \leq 0.0001$ were determined by ANOVA followed by Tukey's or Games–Howell post hoc comparison test.

Palmitic Acid Caused Injury to Murine Renal Mesangial Cells. Coculture of murine renal mesangial cells (mRMCs) with palmitic acid (PA) resulted in an increase in the mRNA level of *Mcp-1* both time- and dose-dependently (Fig. 3*A*). In addition, mRMCs treated with PA at both 100 and 300 μM for 9 h and longer resulted in visual damage to the mRMCs, such as morphological deformity and the decrease in cell density and transparency compared with the control mRMCs.

PA Inactivated Pax2 and Ampk in the mRMCs. Treatment with PA at both 100 and 300 μM for 6 h resulted in a significant decrease in the mRNA level of *Ampk* in mRMCs, but nonsignificant difference was observed in the mRMCs cocultured for 3 h or 9 h (Fig. 3*B*). Also, treatment with PA at both 100 and 300 μM for 6 and 9 h led to a significant decrease in the mRNA level of *Pax2* in mRMCs but only a slight change when cocultured for 3 h (Fig. 3*C*). PA treatment significantly decreased the protein levels of p-Ampk$_\alpha$ and Pax2 in mRMCs when cocultured for 6 h (*SI Appendix*, Fig. S8).

Epoxy Fatty Acids Attenuated PA-Mediated mRMCs Injury. The administration of epoxy fatty acids (EpFAs) including 9(10)- and 12(13)-epoxyoctadecenoic acid (EpOME), as well 5(6)-, 8(9)-, 11(12)-, and 14(15)-EET, at 100 nM to PA-treated mRMCs all significantly inhibited PA-induced increase in *Mcp-1* (Fig. 3*D*). In addition, 14(15)-EET reduced PA-induced increase in *Mcp-1* dose-dependently (Fig. 3*D*).

The Effects of EpFAs and 14,15-DHET on *Pax2* and *Ampk* in PA-Mediated mRMCs. The administration of 12(13)-EpOME or 5(6)- or 14(15)-EET at 100 nM to PA-treated mRMCs all significantly reversed PA-induced decrease in *Ampk* (Fig. 3*E*). Also, the treatment of 5(6)-, 8(9)-, or 14(15)-EET at 100 nM to PA-treated mRMCs significantly reversed PA-induced decrease in *Pax2* (Fig. 3*F*). In addition, 14(15)-EET but not 14,15-DHET treatment significantly increased the PA-induced inactivation of p-Ampk$_\alpha$, Pax2, and p-Pax2 in protein levels in the mRMCs (Fig. 3 *G*–*J* and *SI Appendix*, Fig. S7 *C* and *D*).

Pax2 Positively Regulated Ampk in Vitro. Small hairpin (*sh*) RNA interference and overexpression (*oe*) of *Pax2* and *Ampk* by plasmid construction were used to investigate the possible relations between *Pax2* and *Ampk*. Interestingly, even under normative status, targeted silencing and overexpression of *Pax2* and *Ampk* increased *Mcp-1* in the transfected mRMCs, compared with their respective controls (Fig. 4 *A* and *D*). As expected, forced encoding of the mRMCs with the constructed plasmids (*shAmpk*, *shPax2*, *oeAmpk*, and *oePax2*) decreased or increased, respectively, the mRNA and protein's expression of the targets (Fig. 4 *B*, *C*, *E*–*L*). Unexpectedly, the transfection with *shPax2* and *oePax2* significantly down-regulated and up-regulated Ampk at both mRNA (Fig. 4 *B* and *E*) and protein (Fig. 4 *H* and *K*) levels, respectively, in the mRMCs. In contrast, forced encoding of the mRMCs with *shApmk* or *oeAmpk* changed the protein level of Pax2 slightly (Fig. 4 *I* and *L*). However, forced encoding of the mRMCs with *oeAmpk* significantly decreased the mRNA level of *Pax2*, while *shAmpk* decreased it slightly (Fig. 4 *F* and *C*). Furthermore, the treatment of PA with and without 14(15)-EET modified Ampk at mRNA and protein levels in the *shPax2* and *oePax2* transfected mRMCs in a similar pattern to their respective controls (*SI Appendix*, Figs. S9 *A*, *B*, *E*, and *G*). However, in the mRMCs forced encoded with *shAmpk* and *oeAmpk*, the treatment of PA with or without 14(15)-EET only slightly modified *Pax2* at mRNA level (*SI Appendix*, Fig. S9 *C* and *D*), while modifying the Pax2 protein in a similar pattern to their respective controls (*SI Appendix* Fig. S9 *F* and *H*). In addition, compared with the respective controls, forced encoding of the mRMCs with *shAmpk* and *oeAmpk* modified Pax2 at the protein level insignificantly (*SI Appendix* Fig. S9 *F* and *H*).

Discussion

This study revealed that HFD-caused renal injury involves the inactivation of Pax2. Eight-week feeding of an HFD caused renal injury and significant decrease in Pax2 at mRNA and protein levels in murine kidney (Fig. 1*G* and *SI Appendix*, Fig. S4 *E* and *F*).

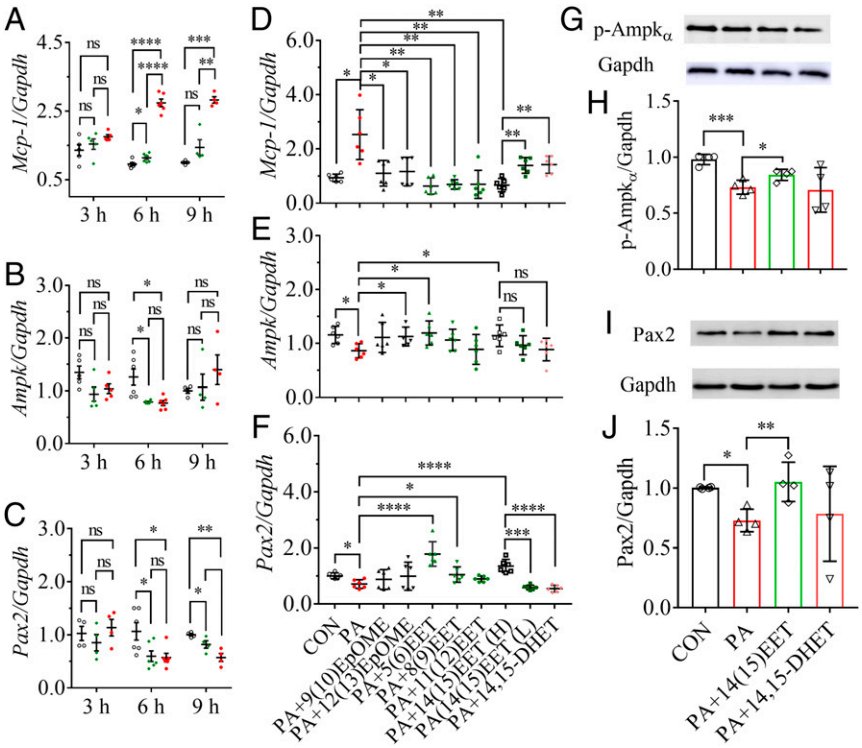

Fig. 3. EpFAs attenuated PA-caused injury to the renal mesangial cells (mRMCs) by activating Pax2 and Ampk. The treatment of PA modified mRNA levels of (*A*) *Mcp-1*, (*B*) *Ampk*, and (*C*) *Pax2* in mRMCs both dose- and time-dependently. For *A*–*C*, unfilled circles, green diamonds, and red dots indicated the mRMCs were treated with PA at 0, 100, and 300 μM, respectively. The high concentration of 14(15)-EET and the concentration of other EpFAs tested were 100 nM, while the lower concentration of 14(15)-EET was 10 nM. Treatment of EpFAs modified PA-mediated mRNA levels of (*D*) *Mcp-1*, (*E*) *Ampk*, and (*F*) *Pax2* in mRMCs. Treatment of 14(15)-EET but not 14,15-DHET significantly reversed the PA-induced decrease of the protein levels of (*G* and *H*) p-Ampk$_\alpha$ and (*I* and *J*) Pax2 in mRMCs ($n = 4$). Treatments of 14(15)-EET and 14,15-DHET to PA-mediated mRMCs resulted in similar changes in protein levels of p-Pax2 to those of Pax2, which were presented in *SI Appendix*, Fig. S7 *C* and *D*. Data represent mean ± SEM for *A*–*F* and mean ± SD for *H* and *J*; ns (no significant difference) $P \geq 0.05$, $0.01 < {}^{*}P < 0.05$, $0.001 < {}^{**}P \leq 0.01$, $0.0001 < {}^{***}P \leq 0.001$, and ${}^{****}P \leq 0.0001$ were determined by two-tailed *t* test for *A*–*F* and ANOVA followed by Tukey's or Games–Howell post hoc comparison test for *H* and *J*.

Furthermore, when the HFD-mediated renal injury was attenuated by the inhibition of sEH (*SI Appendix*, Figs. S5 and S6), the renal Pax2 protein was also significantly up-regulated (Fig. 2*L*). These data suggest that inhibition of sEH attenuated HFD-mediated renal injury by, at least in part, activating Pax2. In addition to acting as a mediator for CMA, Pax2 is also a transcription factor for renal development, whose reactivation in mature cells may lead to multiple renal diseases (36). However, in this model, Pax2 functions most like a CMA mediator, which was supported by a previous study, which found that reduced CMA contributes to diabetes-induced renal hypertrophy (29). In addition, CMA was reported previously to be inhibited by an HFD, although Pax2 was not discussed in that study (24). Therefore, the feeding of an HFD may ablate the CMA partially by inactivating Pax2, contributing to the onset and progress of renal hypertrophy. The role of Pax2 as a CMA mediator in HFD-mediated renal injury was reported in the present study, although it was previously reported to be inactivated in renal dysfunction in a Zucker rat model of obesity (37, 38), which, in turn, supports the findings in this study. In addition, p-Pax2 changed in a similar pattern to Pax2 response to the treatments in vivo and in vitro (*SI Appendix*, Figs. S7 and S10 *D*, *G*, and *H*), suggesting that treatment with an HFD, an sEH inhibitor, or 14(15)-EET may modify Pax2, rather than its phosphorylation.

This study also demonstrated that sEH plays a crucial role in HFD-mediated renal injury. On the one side, HFD-mediated

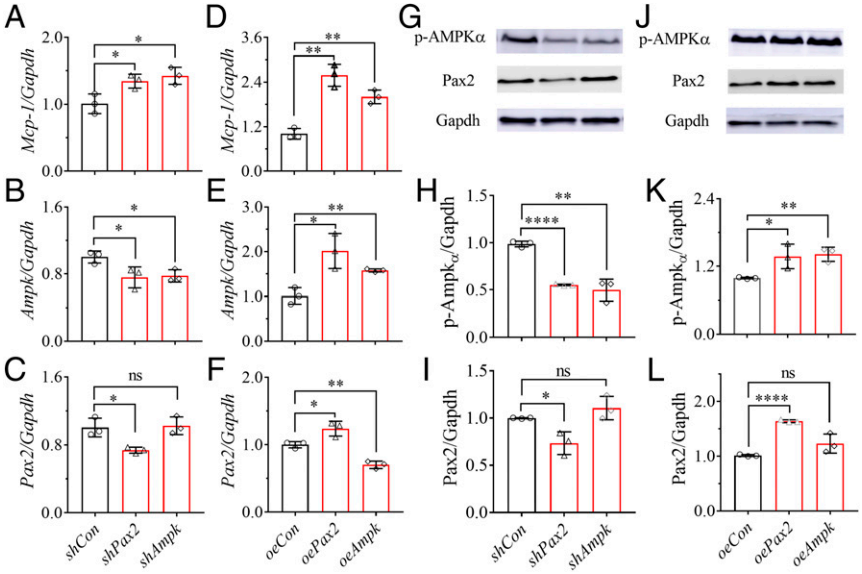

Fig. 4. Pax2 positively regulates Ampk in the mRMCs. Forced encoding of mRMCs with *shPax2*, *oePax2*, *shAmpk*, and *oeAmpk* modified the (*A* and *D*) *Mcp-1*, (*B* and *E*) *Ampk*, and (*C* and *F*) *Pax2* at mRNA levels under normative status. (*G*–*L*) Western blot analysis and quantitation of the band density of (*G*, *J*, *H*, and *K*) p-Ampk$_\alpha$ and (*G*, *J*, *I*, and *L*) Pax2 for the mRMCs transfected with *shPax2*, *oePax2*, *shAmpk*, *oeAmpk*, and their controls for 48 h. The changes in Pax2 and Ampk at mRNA and protein levels in the transfected mRMCs treated with PA with or without 14(15)-EET were presented in *SI Appendix*, Fig. S9. Data represent mean ± SD ($n = 3$); ns (no significant difference) $P \geq 0.05$, $0.01 < {}^{*}P < 0.05$, $0.001 < {}^{**}P \leq 0.01$, and ${}^{****}P \leq 0.0001$ were determined by two-tailed *t* test.

renal injury led to the increased expression of sEH. A metabolic profiling of LSMs of the renal cortex from the mice fed with an HFD and a CTD for 8 wk located that 5,6-, 8,9-, and 11,12-DHET were the markers in the HFD-mediated renal injury by an S plot (Fig. 1*B*) and variable importance for projection (VIP) values (*SI Appendix*, Table S1) in the OPLS-DA model. Further analyses then focused on DHETs and their sEH-mediated precursors, EETs (Fig. 1*C* and *SI Appendix*, Fig. S2*I*). Since the changes in renal EETs and DHETs may result from the changes in Cyp2c, Cyp2j, and/or sEH (Fig. 1*F*), we performed the qPCR analyses of these genes in the renal cortex. As a result, the activation of sEH was found to be the major factor responsible for the changes in renal EETs and DHETs (Fig. 1*I* and *SI Appendix*, Fig. S2*J*), which was also supported by the immunoblot analysis of the renal sEH (*SI Appendix*, Fig. S4 *A* and *B*). The changes in renal 19(20)-EDP/19,20-DiHiDPE ratio (*SI Appendix*, Figs. S2*K* and S5*G* and Tables S4 and S5) and the sum of the renal EpFAs and their respective diol metabolites (*SI Appendix*, Tables S1 and S2) also support that the activity of renal sEH but not *Cyp2c* and *Cyp2j* was increased by an HFD. Thus, the sEH appears to be a marker of inflammation associated with the actions of an HFD on the kidney. On the other side, inhibition of sEH can attenuate HFD-mediated renal injury (*SI Appendix*, Figs. S5 and S6). The inhibition of sEH by the treatment of TPPU was demonstrated by the significant changes at mRNA and protein levels, as well as the changes in the renal levels of EETs and DHETs as anticipated (Fig. 2 *D*–*F*). Our data suggest that TPPU may, at least in part, inhibit sEH transcriptionally. The activation of sEH by an HFD was consistent with a previous study reported by Bettaieb et al. (39). However, the changes in renal EETs and DHETs are different from another previous study (40), in which Theken et al. reported that an HFD failed to significantly modify the renal levels of EETs and DHETs. This may be accounted for by the different HFDs used in two studies, a 21% fat diet used in the previous study while a 60% kcal% fat diet was used in the present study. Roche et al. (41) also reported different results in renal EETs and DHETs than those caused by an HFD in this study, which may be accounted for by the different animal models used. The previous study employed FVB/N mice, but this study used C57BL/6 mice.

Besides the EpFAs and diols, renal TXB_2 was also decreased after an HFD treatment, and this decrease was reversed by TPPU treatment (*SI Appendix*, Tables S1 and S2). This may be because an HFD treatment stimulates inflammation and thus increases the metabolism of TXB_2. This hypothesis was supported by the facts that renal *Il-6* was changed upon an HFD treatment with or without TPPU as expected, and the liver level of 2,3-dinor-TXB_2, the major metabolite of TXB_2, was significantly higher in HFD-treated mice than those of CTD-treated mice (28.4 ± 4.4 vs. 23.3 ± 5.2, $P = 0.0082$). In addition, renal levels of 15-, 11-, 9-, 8-, and 5-HETE were lower in HFD-treated mice than those of CTD-treated mice (*SI Appendix*, Table S1). Since these HETEs are the metabolites of ARA mediated by lipoxygenases (LOXs) and some CYP monooxygenases. The renal LTB_4 and 6-*trans*-LTB_4 changed slightly upon HFD treatment, which indicates that 5-LOX changed slightly by HFD treatment. Therefore, HFD treatment may blunt some CYP monooxygenases that mediate the biosynthesis of hydroxyeicosatetrasanoic acids (HETEs), and such effects could be enhanced by TPPU treatment (*SI Appendix*, Table S2).

Previous studies reported that Ampk is inactivated in murine kidney by an HFD (21) and the activation of Ampk can attenuate HFD-mediated renal injury (26, 42). In addition, target gene disruption of sEH was reported to activate renal Ampk in a murine model of streptozotocin-induced diabetic nephropathy (43). However, this study revealed that inhibition of sEH attenuated HFD-mediated renal injury involved in the activation of Ampk, which was supported by the fact that the treatment with TPPU significantly increased the mRNA level of *Ampk* (Fig. 2*G*), and its protein level as well (Fig. 2 *H* and *I*).

This study uncovered that the benefit of sEH inhibition to HFD-mediated renal injury may be due to the increased renal EETs activating Pax2 and Ampk. To test the major molecular changes caused by TPPU treatment, we performed an OPLS-DA analysis of the renal LSMs of the mice fed on an HFD with or without TPPU. As a result, 14(15)- and 11(12)-EET were found to be the major molecules that discriminated the two groups (*SI Appendix*, Fig. S11), which was also supported by ANOVA results presented in *SI Appendix*, Table S2. Then a PA-treated mRMCs model was used as in a previous study (21) to test the function of EpFAs. All of the tested EpFAs including two EpOME and four EET regioisomers (100 nM) significantly attenuated the PA-caused increase in *Mcp-1* in the mRMCs (Fig. 3*D*). However, only 5(6)- and 14(15)-EET significantly compressed the PA-induced decrease in both *Pax2* and *Ampk* (Fig. 3 *E* and *F*). So, we used 14(15)-EET as the representative compound for further study. The 14(15)-EET significantly attenuated PA-caused mRMCs injury (Fig. 3*D*) and reversed the PA-caused decrease in Pax2 and Ampk at both mRNA (Fig. 3 *E* and *F*) and protein levels (Fig. 3 *G*–*J*). In contrast, 14,15-DHET, the sEH-mediated metabolite of 14(15)-EET, failed in protecting mRMCs against PA-treatment, and activating Pax2 and Ampk (Fig. 3 *D*–*J*). Also, the effects of 14(15)-EET and 14,15-DHET on the PA-treated murine renal tubular epithelial cells (mRTECs) were similar to those on PA-mediated mRTECs (*SI Appendix*, Fig. S10). In addition, the beneficial effects of 14(15)-EET on mRMCs were blunted by coadministration of 14,15-EE-5(Z)E, an antagonist of 14(15)-EET (*SI Appendix*, Fig. S12). These data, to a large degree, could explain that decreased EpFAs caused by the activation of sEH may result in the inactivation of Pax2 and Ampk, which led to the slowed autophagy and then renal hypertrophy and renal dysfunction. In contrast, inhibition of sEH attenuated HFD-mediated renal injury by increased EETs activating the Pax2-mediated CMA and Ampk-mediated autophagy. Also, HFD-caused time course increase in plasma glucose (*SI Appendix*, Fig. S2*H*), and such increase was reduced by TPPU treatment nonsignificantly (*SI Appendix*, Fig. S5*F*). In addition, TPPU treatment significantly attenuated renal *Il-6* (*SI Appendix*, Fig. S5*D*). Previously, sEH inhibition was reviewed to be antiinflammatory, antihypertensive, and antidiabetic (35). Taken together, these effects of sEH inhibition may contribute to the activation of Ampk and Pax2, and the renoprotection by increased EETs.

To test the possible relationships between *Pax2* and *Ampk*, we adopted the mRMCs transfected with the plasmids that targeted silence of *Pax2* (*shPax2*) or *Ampk* (*shAmpk*), and overexpression of Pax2 (*oePax2*) or Ampk (*oeAmpk*), respectively. Forced encoding with *shPax2* or *oePax2* resulted in the change in mRNA and protein levels of Ampk parallel to Pax2 (Figs. 4 *B*, *E*, *H*, and *K*), suggesting that Pax2 may regulate Ampk positively. Also, the mRNA and protein Ampk in the mRMCs treated with *shPax2* or *oePax2* responded to the treatment of PA with or without 14(15)-EET in a similar pattern to those of their respective controls (*SI Appendix*, Figs. S9 *A*, *B*, *E*, and *G*), which, to a certain degree, supports that Pax2 may regulate Ampk positively. However, these data also suggest the possibility that Ampk may be regulated, in part, by factors other than Pax2. For example, Ampk may be partially regulated by EETs directly. In addition, protein Pax2 in the mRMCs transfected with *shAmpk* or *oeAmpk* responded to PA with or without PA treatment in a similar pattern to those for the respective controls, although the mRNA level of *Pax2* in the *shAmpk* and *oeAmpk* transfected mRMCs failed in response to PA with or without 14(15)-EET (*SI Appendix*, Figs. S9 *C*, *D*, *F*, and *H*), which suggests that Ampk regulation may be downstream of Pax2 at the protein level. This was also supported by the change in renal *Pax2* that occurred earlier than that of *Ampk* (Fig. 1 *G* and *H*). Pax2 protein mainly presents inside the nuclei and is degraded to trigger the CMA

when it presents outside the nuclei (*SI Appendix*, Fig. S13) while Ampk protein presents in both the nuclei and cytoplasm (44, 45). Since the regulation of Ampk by Pax2 was clear at both mRNA and protein levels, we think it most likely that Pax2 positively regulates Ampk transcriptionally in murine kidney. Our data reveal the interaction between Pax2 and Ampk, suggesting the profound crosstalk between macroautophagy and CMA, which opens the possibility to better understand the physiology and pathophysiology of other organs where both Pax2 and Ampk are present, like cerebral cortex, colon, bladder, testis, and epididymis.

In summary, this study revealed that (*i*) HFD-mediated kidney injury involves in the inactivation of Pax2 and Ampk, and the activation of sEH, (*ii*) inhibition of sEH attenuates the HFD-mediated renal injury through, at least in part, the increased EETs activating of Pax2 and Ampk, and (*iii*) Pax2 may positively regulate Ampk transcriptionally (*SI Appendix*, Fig. S14). In short, this study provides insights into the HFD-mediated renal injury. Targeting activation of Pax2 and Ampk, as well as an increase of EET levels by pharmacological interventions like sEH inhibition, may offer therapies for the HFD-mediated renal injury and other associated diseases.

Materials and Methods

All animal experiments were performed according to the protocols approved by the Animal Use and Care Committee of Shanghai Tenth People's Hospital, Tongji University School of Medicine. The mice had access to CTD or HFD and water ad libitum for 2, 4, or 8 wk. CTD (10 kcal% fat, D12450J) and HFD (60 kcal% fat, D12492J) were purchased from Research Diets, Inc. TPPU was provided in drinking water at a concentration of 10 mg/L. The group information is presented in Figs. 1 and 2. The details of materials, experimental protocols, and analytical methods are presented in *SI Appendix*.

ACKNOWLEDGMENTS. This study was supported, in part, by National Natural Science Foundation of China (NSFC) Grants 81470588, 81672938, and 81602944, as well as National Institute of Environmental Health Sciences (NIEHS) Grant R01 ES02710, NIEHS Superfund Grant P42 ES04699, NIH/National Heart, Lung, and Blood Institute (NHLBI) Grant R01 HL59699-06A1, and a Translational Technology Grant from the University of California, Davis Medical Center.

1. Tilman D, Clark M (2014) Global diets link environmental sustainability and human health. *Nature* 515:518–522.
2. Tracy SW (2013) Something new under the sun? The Mediterranean diet and cardiovascular health. *N Engl J Med* 368:1274–1276.
3. Miller G (2006) Mental health in developing countries. A spoonful of medicine–And a steady diet of normality. *Science* 311:464–465.
4. Wilson CR, Tran MK, Salazar KL, Young ME, Taegtmeyer H (2007) Western diet, but not high fat diet, causes derangements of fatty acid metabolism and contractile dysfunction in the heart of Wistar rats. *Biochem J* 406:457–467.
5. Halton TL, et al. (2006) Potato and french fry consumption and risk of type 2 diabetes in women. *Am J Clin Nutr* 83:284–290.
6. Nystrom FH, et al. (2011) A high fat diet improves glycaemic control compared with low fat diet: A 24-month randomised prospective study of patients with type 2 diabetes in primary health care. *Diabetologia* 54:S358.
7. Yan ZH, Welscher A, Remedi MS (2016) High-fat diet improves blood glucose control in a mouse model of human neonatal diabetes: Protection by fat? *J Gen Physiol* 148: 35a–36a.
8. Duda MK, O'Shea KM, McElfresh TA, Hoit BD, Stanley WC (2007) A high fat diet, but not a high sucrose diet, prevents pressure overload induced cardiac dysfunction and hypertrophy. *FASEB J* 21:A1254–A1255.
9. Zinn C, et al. (2017) A 12-week low-carbohydrate, high-fat diet improves metabolic health outcomes over a control diet in a randomised controlled trial with overweight defence force personnel. *Appl Physiol Nutr Metab* 42:1158–1164.
10. Field AE, Willett WC, Lissner L, Colditz GA (2007) Dietary fat and weight gain among women in the Nurses' Health Study. *Obesity (Silver Spring)* 15:967–976.
11. Garg A (1998) High-monounsaturated-fat diets for patients with diabetes mellitus: A meta-analysis. *Am J Clin Nutr* 67(3, Suppl):577S–582S.
12. Benham V, Bernard JJ (2018) Why does a high-fat diet increase cancer risk? *Future Oncol* 14:583–588.
13. Asou Y, et al. (2016) Pleiotropic functions of high fat diet in the etiology of osteoarthritis. *PLoS One* 11:e0162794.
14. Anand N, et al. (2017) The effect of a high-fat diet on arthritis using a mouse model of rheumatoid arthritis. *J Rheumatol* 44:870–871.
15. Li WG, Prakash R, Ma HD, Ergul A (2013) High fat diet worsens long term stroke outcome. *Stroke,* 44:ATP273.
16. Schwingshackl L, Hoffmann G (2013) Comparison of effects of long-term low-fat vs high-fat diets on blood lipid levels in overweight or obese patients: A systematic review and meta-analysis. *J Acad Nutr Diet* 113:1640–1661.
17. Wang W, et al. (2018) Lipidomic profiling reveals soluble epoxide hydrolase as a therapeutic target of obesity-induced colonic inflammation. *Proc Natl Acad Sci USA* 115:5283–5288.
18. Timmermans S, et al. (2014) High fat diet exacerbates neuroinflammation in an animal model of multiple sclerosis by activation of the renin angiotensin system. *J Neuroimmune Pharmacol* 9:209–217.
19. Morgan K, Mao L, French SW, Morgan TR (2003) Fatty liver and histologic features of non-alcoholic steaohepatitis (NASH) develop in male mice fed a nutritionally comlete high fat diet. *Hepatology* 38:501a.
20. Picchi MG, et al. (2011) A high-fat diet as a model of fatty liver disease in rats. *Acta Cir Bras* 26:25–30.
21. Declèves AE, Mathew AV, Cunard R, Sharma K (2011) AMPK mediates the initiation of kidney disease induced by a high-fat diet. *J Am Soc Nephrol* 22:1846–1855.
22. Fitzgerald SM, Henegar JR, Brands MW, Henegar LK, Hall JE (2001) Cardiovascular and renal responses to a high-fat diet in Osborne-Mendel rats. *Am J Physiol Regul Integr Comp Physiol* 281:R547–R552.
23. Koga H, Kaushik S, Cuervo AM (2010) Inhibitory effect of intracellular lipid load on macroautophagy. *Autophagy* 6:825–827.
24. Rodriguez-Navarro JA, et al. (2012) Inhibitory effect of dietary lipids on chaperone-mediated autophagy. *Proc Natl Acad Sci USA* 109:E705–E714.
25. Jeon SM (2016) Regulation and function of AMPK in physiology and diseases. *Exp Mol Med* 48:e245.
26. Sohn M, et al. (2017) Delayed treatment with fenofibrate protects against high-fat diet-induced kidney injury in mice: The possible role of AMPK autophagy. *Am J Physiol Renal Physiol* 312:F323–F334.
27. Declèves AE, et al. (2014) Regulation of lipid accumulation by AMP-activated kinase [corrected] in high fat diet-induced kidney injury. *Kidney Int* 85:611–623.
28. Shen W, Brown NS, Finn PF, Dice JF, Franch HA (2006) Akt and mammalian target of rapamycin regulate separate systems of proteolysis in renal tubular cells. *J Am Soc Nephrol* 17:2414–2423.
29. Sooparb S, Price SR, Shaoguang J, Franch HA (2004) Suppression of chaperone-mediated autophagy in the renal cortex during acute diabetes mellitus. *Kidney Int* 65:2135–2144.
30. Franch HA, Sooparb S, Du J, Brown NS (2001) A mechanism regulating proteolysis of specific proteins during renal tubular cell growth. *J Biol Chem* 276:19126–19131.
31. Wang B, Zeng H, Wen Z, Chen C, Wang DW (2016) CYP2J2 and its metabolites (epoxyeicosatrienoic acids) attenuate cardiac hypertrophy by activating AMPKα2 and enhancing nuclear translocation of Akt1. *Aging Cell* 15:940–952.
32. Zhang S, et al. (2015) CYP2J2 overexpression ameliorates hyperlipidemia via increased fatty acid oxidation mediated by the AMPK pathway. *Obesity (Silver Spring)* 23: 1401–1413.
33. Samokhvalov V, et al. (2013) Epoxyeicosatrienoic acids protect cardiac cells during starvation by modulating an autophagic response. *Cell Death Dis* 4:e885.
34. Zhang G, Kodani S, Hammock BD (2014) Stabilized epoxygenated fatty acids regulate inflammation, pain, angiogenesis and cancer. *Prog Lipid Res* 53:108–123.
35. Morisseau C, Hammock BD (2013) Impact of soluble epoxide hydrolase and epoxyeicosanoids on human health. *Annu Rev Pharmacol Toxicol* 53:37–58.
36. Sharma R, Sanchez-Ferras O, Bouchard M (2015) Pax genes in renal development, disease and regeneration. *Semin Cell Dev Biol* 44:97–106.
37. Ndisang JF, Tiwari S (2015) Featured article: Induction of heme oxygenase with hemin improves pericardial adipocyte morphology and function in obese Zucker rats by enhancing proteins of regeneration. *Exp Biol Med (Maywood)* 240:45–57.
38. Ndisang JF, Tiwari S (2014) Mechanisms by which heme oxygenase rescue renal dysfunction in obesity. *Redox Biol* 2:1029–1037.
39. Bettaieb A, et al. (2017) Soluble epoxide hydrolase in podocytes is a significant contributor to renal function under hyperglycemia. *Biochim Biophys Acta Gen Subj* 1861: 2758–2765.
40. Theken KN, et al. (2012) Enalapril reverses high-fat diet-induced alterations in cytochrome P450-mediated eicosanoid metabolism. *Am J Physiol Endocrinol Metab* 302: E500–E509.
41. Roche C, et al. (2015) Impact of soluble epoxide hydrolase inhibition on early kidney damage in hyperglycemic overweight mice. *Prostaglandins Other Lipid Mediat* 120: 148–154.
42. Zhang SQ, et al. (2014) Protective effect of metformin on renal injury of C57BL/6J mouse treated with high fat diet. *Pharmazie* 69:904–908.
43. Chen G, et al. (2012) Genetic disruption of soluble epoxide hydrolase is protective against streptozotocin-induced diabetic nephropathy. *Am J Physiol Endocrinol Metab* 303:E563–E575.
44. Kodiha M, Rassi JG, Brown CM, Stochaj U (2007) Localization of AMP kinase is regulated by stress, cell density, and signaling through the MEK–>ERK1/2 pathway. *Am J Physiol Cell Physiol* 293:C1427–C1436.
45. Miyamoto T, et al. (2015) Compartmentalized AMPK signaling illuminated by genetically encoded molecular sensors and actuators. *Cell Rep* 11:657–670.